Inhibition of Integrin-Linked Kinase Attenuates Renal Interstitial Fibrosis

Yingjian Li,* Xiaoyue Tan,* Chunsun Dai,* Donna B. Stolz,† Dan Wang,* and Youhua Liu*

Departments of *Pathology and †Cell Biology and Physiology, University of Pittsburgh School of Medicine, Pittsburgh, Pennsylvania

ABSTRACT

Integrin-linked kinase (ILK) is an intracellular serine/threonine protein kinase that regulates cell adhesion, survival, and epithelial-to-mesenchymal transition (EMT). In this study, we investigated the kinase activity of ILK during tubular EMT induced by TGF-β1 and examined the therapeutic potential of an ILK inhibitor in obstructive nephropathy. TGF-β1 induced a biphasic activation of ILK in renal tubular epithelial cells, with rapid activation starting at 5 min and the second wave of activation peaking at 24 h; the latter paralleled the induction of ILK protein expression. Pharmacologic inhibition of ILK with small-molecule inhibitor QLT-0267 abolished TGF-β1–induced phosphorylation of Akt and glycogen synthase kinase-3β, suppressed cyclin D1 expression, and largely restored the expression of E-cadherin and zonula occludens 1. Inhibition of ILK also blocked TGF-β1–mediated induction of fibronectin, Snail1, plasminogen activator inhibitor 1, and matrix metalloproteinase 2. In a mouse model of obstructive nephropathy, administration of QLT-0267 inhibited β-catenin accumulation; suppressed Snail1, α-smooth muscle actin, fibronectin, vimentin, and type I and type III collagen expression; and reduced total tissue collagen content. Inhibition of ILK did not affect kidney structure or function in normal mice. These findings suggest that increased ILK activity mediates EMT and the progression of renal fibrosis. Pharmacologic inhibition of ILK signaling may hold therapeutic potential for fibrotic kidney diseases.

J Am Soc Nephrol 20: 1907–1918, 2009. doi: 10.1681/ASN.2008090930

Integrin-linked kinase (ILK) is an intracellular serine/threonine protein kinase that plays a fundamental role in the regulation of cell adhesion, survival, proliferation, and extracellular matrix (ECM) deposition.[1,2] As its name implies, ILK interacts with the cytoplasmic domains of the β integrins and mediates the integrin signaling in diverse types of cells. Structurally, ILK comprises three distinct regions. There are four ankyrin repeats in its N-terminus. A pleckstrin homology–like motif locates at the downstream of ankyrin domain, and the C-terminus of ILK harbors kinase catalytic domain and integrin binding domain.[3,4] These unique features render ILK two principal properties: As a scaffolding protein and as a protein kinase. Through multiple interactions by using distinct domains, ILK strategically connects the integrins with numerous intracellular proteins, such as α-parvin and PINCH (particularly interesting new cysteine-histidine rich protein).[4–6] In addition, the catalytic kinase activity of ILK enables it to phosphorylate directly several physiologically important downstream effector kinases, such as Akt/protein kinase B and glycogen synthase kinase (GSK)-3β.[7,8] By so doing, ILK integrates a diverse array of signal inputs and transmits signal exchanges between the intracellular and extracellular compartments.

Previous studies from this laboratory indicated that ILK is a key intracellular mediator of tubular

Received September 4, 2008. Accepted April 16, 2009.

Published online ahead of print. Publication date available at www.jasn.org.

Correspondence: Dr. Youhua Liu, Department of Pathology, University of Pittsburgh, S-405 Biomedical Science Tower, 200 Lothrop Street, Pittsburgh, PA 15261. Phone: 412-648-8253; Fax: 412-648-1916; E-mail: liuy@upmc.edu

epithelial-to-mesenchymal transition (EMT) induced by TGF-β1.[9] This finding is consistent with several observations that ILK expression is upregulated in a wide variety of chronic kidney diseases in both experimental and clinical settings.[9–12] It is worthwhile to point out that ILK is not only of critical importance in mediating TGF-β1–initiated EMT but is also indispensable in governing EMT induced by other stimuli such as connective tissue growth factor.[13] Furthermore, ILK is independently identified as a key mediator of podocyte dysfunction and proteinuria in many forms of proteinuric kidney diseases,[11,12] wherein podocytes also undergo EMT as recently reported.[14] These results underscore that ILK could be a crucial regulator of EMT and may play an imperative role in the pathogenesis of tissue fibrosis in different circumstances.

The action of ILK in regulating EMT seems to be mediated primarily by its protein kinase activity, as a kinase-dead mutant inhibits TGF-β1–mediated EMT in a dominant negative manner.[9] In view of that ILK phosphorylates GSK-3β and Akt, which directly or indirectly leads to the stabilization of β-catenin and activation of other transcription factors,[12,15] it becomes increasingly clear that ILK controls the activities of several key signaling pathways, leading to the stimulation of their downstream effector kinases and transcription factors, thereby dictating the expression of an array of genes that are required for EMT.[1,16,17] In this context, it is conceivable to speculate that specific inhibition of ILK activity might be effective in blocking EMT and in attenuating renal fibrosis.

In this study, we investigated the ILK kinase activity during tubular EMT induced by TGF-β1 and evaluated the therapeutic potential of ILK inhibitor in mouse model of obstructive nephropathy. Our results suggest that hyperactive ILK plays a crucial role in mediating tubular EMT and the progression of renal fibrosis, and targeting this signaling therefore could be an effective strategy for the treatment of fibrotic kidney disorders.

RESULTS

A Biphasic Activation of ILK Activity during TGF-β1–Induced EMT

We first assessed the kinase activity of ILK in renal tubular epithelial cells during TGF-β1–induced EMT. As shown in Figure 1A, treatment of human proximal tubular epithelial cells (HKC-8) with TGF-β1 induced a rapid increase in ILK activity, as illustrated by an *in vitro* kinase assay. Interestingly, kinetic studies revealed that TGF-β1 activated ILK kinase activity in a biphasic manner. ILK activity started to increase as early as 5 min, then declined to the baseline level at 1 h and reached second peak at 24 h after TGF-β1 treatment (Figure 1, A and B). The latter wave of ILK activation was correlated closely with the ILK protein induction in HKC-8 cells by TGF-β1 (Figure 1, C and D). These results indicate that TGF-β1 not only induces ILK abundance as previously reported[9] but also activates its kinase activity. Furthermore, the early activation of ILK activity elicited by TGF-β1 seems to be independent of its protein induction in tubular epithelial cells.

Small-Molecule Inhibitor QLT-0267 Suppresses ILK Activity and Inhibits Its Downstream Signaling

To evaluate the functionality of ILK activation in EMT process, we used a high selective small-molecule ILK inhibitor,[15,18] QLT-0267, to block ILK signaling. As shown in Figure 2A, *in vitro* kinase assay demonstrates that QLT-0267 inhibited the phosphorylation of myelin basic protein substrate by ILK in a dosage-dependent manner. Effective inhibition of ILK kinase activity by QLT-0267 was found at the concentrations ranging from 1 to 10 μM (Figure 2A).

We next sought to determine whether inhibition of ILK activity by QLT-0267 leads to an attenuated Akt and GSK-3β phosphorylation induced by TGF-β1, because they are known

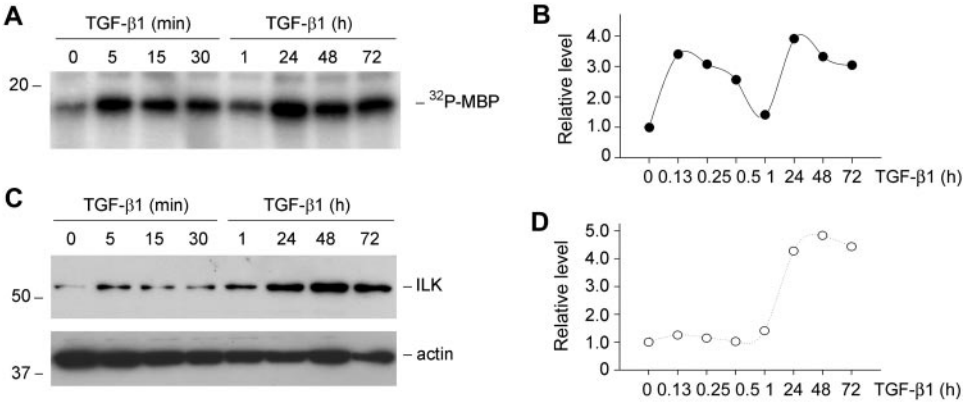

Figure 1. TGF-β1 induces ILK activity in renal tubular epithelial cells. (A and B) *In vitro* kinase assay shows that TGF-β1 induced a biphasic activation of ILK kinase activity. HKC-8 cells were incubated with TGF-β1 at the concentration of 2 ng/ml for various periods of time as indicated. Total cell lysates were immunoprecipitated with polyclonal anti-ILK antibody. Kinase assay was performed using myelin basic protein (MBP) as the substrate. (A) Representative assay. (B) Graphic presentation of the kinetics of ILK activation. (C and D) TGF-β1 also induced ILK expression in a delayed manner. Total cell lysates were immunoblotted with specific antibodies against ILK and actin, respectively. (C) Representative Western blot. (D) Graphic presentation of relative ILK protein levels (fold induction *versus* controls).

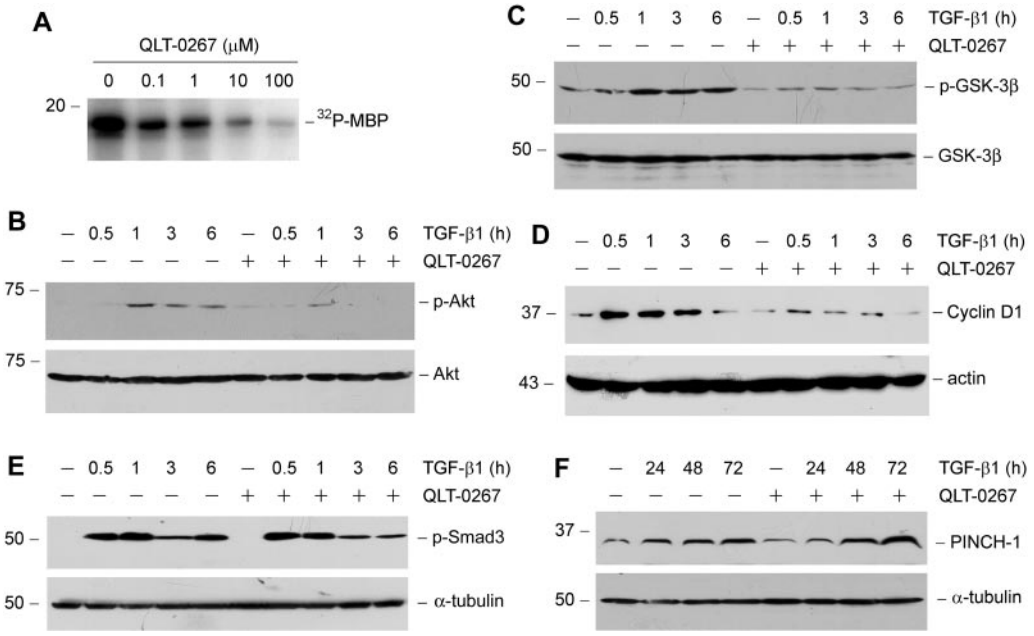

Figure 2. Small-molecule inhibitor QLT-0267 suppresses ILK activity and inhibits its downstream signaling. (A) *In vitro* kinase assay demonstrates that QLT-0267 inhibited ILK activity in a dosage-dependent manner. ILK was immunoprecipitated from HKC-8 cell lysate, and *in vitro* kinase assay was performed in the absence or presence of QLT-0267 at various concentrations as indicated. (B through D) Inhibition of ILK activity reduces the TGF-β1–triggered Akt phosphorylation, GSK-3β phosphorylation, and cyclin D1 expression. HKC-8 cells were pretreated with or without QLT-O267 (10 μM) for 1 h and then incubated with TGF-β1 (2 ng/ml) for different periods as indicated. Cell lysates were immunoblotted with antibodies against phospho- or total Akt (B), phospho- or total GSK-3β (C), and cyclin D1 and actin (D), respectively. (E) Inhibition of ILK activity does not affect the TGF-β1–triggered Smad3 phosphorylation. Cell lysates were immunoblotted with antibodies against phospho-Smad3 or α-tubulin, respectively. (F) Inhibition of ILK activity does not affect the TGF-β1–induced PINCH-1 expression. HKC-8 cells were treated with or without QLT-O267 (5 μM) in the absence or presence of TGF-β1 (2 ng/ml) for different periods as indicated.

ILK downstream targets.[1,2] As shown in Figure 2B, TGF-β1 induced phosphorylation of Akt on Ser473 in HKC-8 cells, which was blunted by co-incubation with QLT-0267. Similarly, inhibition of ILK activity by QLT-0267 also blocked the TGF-β1–triggered phosphorylation of GSK-3β on Ser9 in HKC-8 cells (Figure 2C). GSK-3β phosphorylation would cause its inactivation, leading to its downstream β-catenin stabilization and subsequent nuclear translocation, which activates the expression of β-catenin target genes such as cyclin D1. We further examined the effect of ILK inhibition on cyclin D1 expression. As shown in Figure 2D, TGF-β1 induced cyclin D1 expression in HKC-8 cells, and QLT-0267 almost completely blocked cyclin D1 induction. Inhibition of ILK activity by QLT-0267, however, did not affect TGF-β1–mediated Smad3 phosphorylation (Figure 2E). QLT-0267 also did not abolish PINCH-1 induction by TGF-β1 (Figure 2F), which is dependent on Smad signaling.[6] Together, it is clear that small-molecule inhibitor QLT-0267 specifically blocks ILK signaling in tubular epithelial cells.

Inhibition of ILK Activity Blocks Tubular EMT

We further examined the ability of ILK inhibitor in preserving tubular epithelial cell phenotype. After TGF-β1 treatment, HKC-8 cells underwent transformation from typical cobblestone morphology into the spindle-shaped, fibroblast-like appearance (Figure 3, A and B). Simultaneous incubation with QLT-0267 and TGF-β1, however, largely preserved the epithelial morphology of HKC-8 cells (Figure 3C). We further investigated the expression of zonula occludens 1 (ZO-1) and E-cadherin, two epithelial adhesion proteins that play a crucial role in the maintenance of epithelial integrity.[19,20] As illustrated in Figure 3E, treatment of HKC-8 cells with TGF-β1 resulted in loss of ZO-1 protein at the cell–cell junctions, as shown by an indirect immunofluorescence staining. Co-incubation with TGF-β1 and QLT-0267, however, largely restored ZO-1 protein staining (Figure 3F). Similarly, TGF-β1 dramatically repressed E-cadherin expression in HKC-8 cells, and QLT-0267 was able to restore, at least partially, the TGF-β1–repressed E-cadherin expression (Figure 3G). Hence, inhibition of ILK activity by QLT-0267 is able to preserve tubular epithelial cell phenotype after TGF-β1 treatment.

One of the cellular consequences of EMT is the excessive production of interstitial matrix components, such as fibronectin.[20] As shown in Figure 3I, immunofluorescence staining displayed a dramatic increase in fibronectin deposition by HKC-8 cells after TGF-β1 treatment. Fibronectin was deposited and properly assembled in the extracellular compartment. Inhibition of ILK activity by QLT-0267 substantially

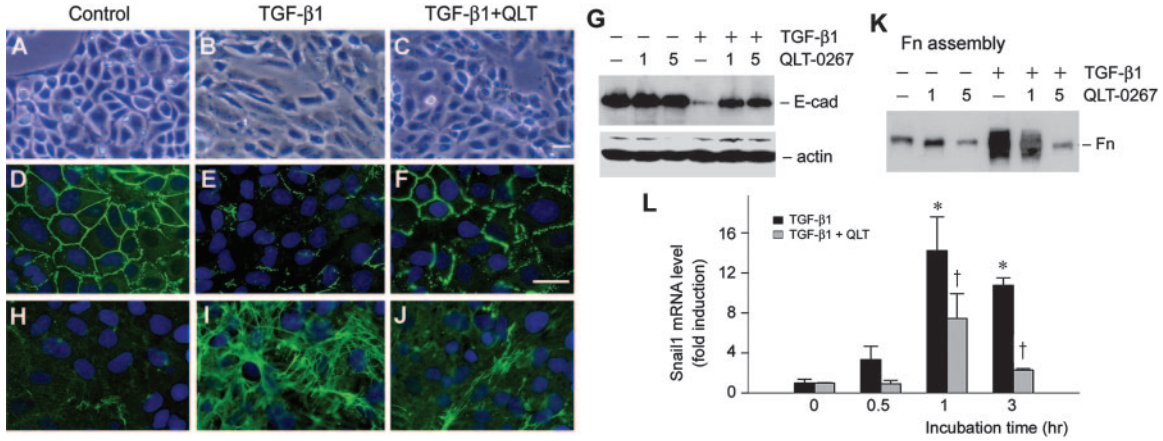

Figure 3. Inhibition of ILK restores epithelial ZO-1 and E-cadherin and inhibits fibronectin and Snail1 expression after TGF-β1 treatment. (A through C) Inhibition of ILK by QLT-0267 preserved the epithelial morphology of HKC-8 cells after TGF-β1 treatment. (D through F) Indirect immunofluorescence staining shows that QLT-0267 treatment restored ZO-1 expression in HKC-8 cells. (H through J) QLT-0267 treatment suppressed the TGF-β1–induced fibronectin expression and its deposition at the extracellular space. (A, D, and H) control. (B, E, and I) TGF-β1 (2 ng/ml). (C, F, and J) TGF-β1 plus QLT-0267 (5 μM). Bar = 20 μm. (G) Western blot analysis demonstrates that QLT-0267 restored E-cadherin expression after treatment with TGF-β1 in HKC-8 cells. HKC-8 cells were incubated with or without TGF-β1 (1 ng/ml) in the absence or presence of different amounts of QLT-0267 as indicated for 48 h. E-cad, E-cadherin. (K) Inhibition of ILK by QLT-0267 reduced the extracellular assembly of fibronectin after TGF-β1 treatment. Extracellular protein extracts were prepared after various treatments as indicated and subjected to Western blot analyses using fibronectin antibody. Fn, fibronectin. (L) Inhibition of ILK suppressed the EMT-regulatory gene Snail1 expression. Snail1 mRNA levels were assessed by quantitative real-time RT-PCR in HKC-8 cells after various treatments as indicated.

impeded fibronectin deposition induced by TGF-β1 (Figure 3J). We further examined the extracellular assembly of fibronectin by a quantitative, biochemical assay of the abundance of fibronectin in the ECM preparations.[9,21] As demonstrated in Figure 3K, TGF-β1 dramatically increased fibronectin assembly in the extracellular compartment, whereas co-incubation with QLT-0267 completely blocked the TGF-β1–induced fibronectin assembly. Of note, QLT-0267 also blocked the induction of total fibronectin expression by TGF-β1 in HKC-8 cells, as shown by Western blot analysis (data not shown).

Snail1 is a transcription factor that plays a critical role in regulating EMT by downregulating E-cadherin expression.[22,23] As shown in Figure 3L, Snail1 mRNA was markedly induced by TGF-β1 in HKC-8 cells; however, QLT-0267 largely blunted Snail1 induction. Hence, it seems that inhibition of ILK activity represses a key EMT-regulatory gene.

Inhibition of ILK Represses the TGF-β1–Mediated Plasminogen Activator Inhibitor 1 and Matrix Metalloproteinase 2 Expression

We also investigated the effects of ILK inhibition on the expression of several fibrosis-related genes after TGF-β1 treatment. Plasminogen activator inhibitor 1 (PAI-1) is widely known for its ability to promote the progression of chronic kidney diseases.[24] As shown in Figure 4, A through C, TGF-β1 dramatically induced PAI-1 mRNA and protein expression in HKC-8 cells, and QLT-0267 inhibited PAI-1 induction in a dosage-dependent fashion. Similarly, TGF-β1 induced the steady-state mRNA level of matrix metalloproteinase 2 (MMP-2; Figure 4, D and E), a protease that is both necessary and sufficient for mediating tubular EMT *in vitro*.[25] TGF-β1 also promoted MMP-2 protein expression and secretion (Figure 4F). Co-incubation of HKC-8 cells with QLT-0267, however, dosage-dependently inhibited the induction of MMP-2 by TGF-β1 (Figure 4, D through F). These data clearly indicate that ILK signaling also plays a role in mediating several key fibrosis-related genes such as PAI-1 and MMP-2 induction by TGF-β1.

Inhibition of ILK Activity Does not Affect Normal Kidney Structure and Function In Vivo

We examined the potential effects of ILK inhibitor on glomerular filtration and kidney structure and function in normal mice, because previous studies indicated an important role for ILK in podocyte biology.[26,27] Toward this end, QLT-0267 was administered into mice by daily intraperitoneal injection at 10 mg/kg body wt for 14 d. As presented in Table 1, QLT-0267 affected neither the body and kidney weight nor the urinary albumin and total protein levels. There was no overt abnormality on kidney morphology (Figure 5A). Immunostaining for Wilms' tumor 1 (WT1), nephrin, and podocin revealed no alteration in podocyte numbers and the expression and distribution of major slit diaphragm–associated proteins in mice after inhibition of ILK activity by QLT-0267 (Figure 5A). Electron microscopy also exhibited an intact ultrastructure of podocyte foot processes and glomerular basement membrane after ILK inhibition by QLT-0267 (Figure 5, B and C).

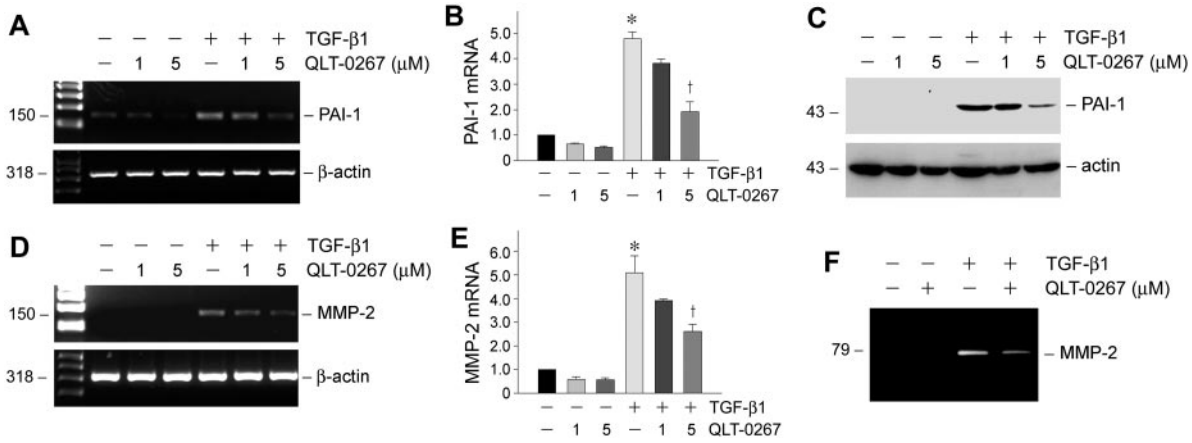

Figure 4. Inhibition of ILK by QLT-0267 abrogates PAI-1 and MMP-2 induction by TGF-β1 in tubular epithelial cells. (A and B) RT-PCR demonstrated a suppressed PAI-1 mRNA expression in HKC-8 cells by QLT-0267. (A) Representative RT-PCR assay. (B) Graphic presentation of PAI-1 mRNA expression in various groups. Data are means ± SEM of three experiments. *$P < 0.05$ *versus* controls; †$P <$ 0.05 *versus* TGF-β1 alone. (C) Western blot demonstrates that QLT-0267 suppressed TGF- β1–induced PAI-1 expression in HKC-8 cells. (D and E) RT-PCR showed that QLT-0267 inhibited MMP-2 mRNA expression in HKC-8 cells. A representative RT-PCR assay (D) and graphic presentation of MMP-2 mRNA expression in various groups (E) are given. *$P < 0.05$ *versus* controls; †$P < 0.05$ *versus* TGF-β1 alone. (F) Zymographic analysis shows the proteolytic activity of MMP-2 in the supernatants of HKC-8 cells after various treatments. The location of MMP-2 is indicated.

Table 1. Body weight, kidney weight, urinary albumin, and total protein level in mice after QLT-0267 administration[a]

Parameter	Body Weight (g)	Kidney Weight (g)	Urinary Albumin (mg/mg Creatinine)	Urinary Total Protein (mg/mg Creatinine)
Vehicle	29.083 ± 0.733	0.414 ± 0.011	0.417 ± 0.055	64.615 ± 6.220
QLT-0267	29.729 ± 0.585	0.412 ± 0.020	0.384 ± 0.049	64.626 ± 12.566

[a]Mice were administered daily injections of vehicle or QLT-0267 at 10 mg/kg body wt for 14 d. Kidney weight represents the sum of two kidneys per mouse. Data are means ± SEM ($n = 5$). There was no statistically significant difference in all parameters between vehicle and QLT-0267 groups.

We also found that administration of QLT-0267 did not affect nephrin and WT1 protein levels in the isolated glomeruli (Figure 5D). Because ILK and nephrin form a ternary protein complex that connects the integrin and slit diaphragm signaling in glomerular podocytes,[27] we next examined whether inhibition of ILK activity affects ILK/nephrin complex formation. As shown in Figure 5E, administration of QLT-0267 *in vivo* did not affect ILK interaction with nephrin, as revealed by co-immunoprecipitation of glomerular lysates. These results suggest that the action of ILK as a scaffolding protein in podocytes is independent of its kinase activity under physiologic conditions.

Inhibition of ILK Activity Reduces β-Catenin Accumulation and Inhibits Snail1 Expression in Obstructive Nephropathy

We next sought to test whether administration of QLT-0267 affects the progression of experimental kidney fibrosis *in vivo*, in view of the effect of ILK inhibitor on blocking tubular EMT *in vitro*. QLT-0267 was administered into mice after unilateral ureteral obstruction (UUO). We first examined the effects of QLT-0267 on renal β-catenin abundance after obstructive injury, because it is a downstream effector of ILK signaling. As shown in Figure 6, A and B, ureteral obstruction caused a >10-fold induction of β-catenin abundance in the kidney, indicating β-catenin activation after injury; however, administration of QLT-026 largely blunted β-catenin induction. Immunohistochemical staining revealed that β-catenin was predominantly localized and accumulated in renal tubules. In addition to localizing at the cell–cell adhesion sites, β-catenin was found in the cytoplasm and nuclei in the obstructed kidney (Figure 6D, arrowheads). Similarly, a much weaker staining for renal β-catenin was observed after QLT-0267 administration (Figure 6E).

Snail1 is a key regulator of EMT and a downstream effector of ILK signaling. Not surprising, inhibition of ILK activity by QLT-0267 *in vivo* also suppressed Snail1 expression in obstructive nephropathy (Figure 6F); therefore, it seems that QLT-0267 can specifically target and block ILK signaling *in vivo*.

Inhibition of ILK Activity Prevents Renal Myofibroblast Activation and Tubular Expression of Mesenchymal Markers In Vivo

We further examined the effects of QLT-0267 on myofibroblast activation after obstructive injury. As shown in Figure 7, A and B, ureteral obstruction induced a marked increase in the expression of α-smooth muscle actin (α-SMA), the molecular

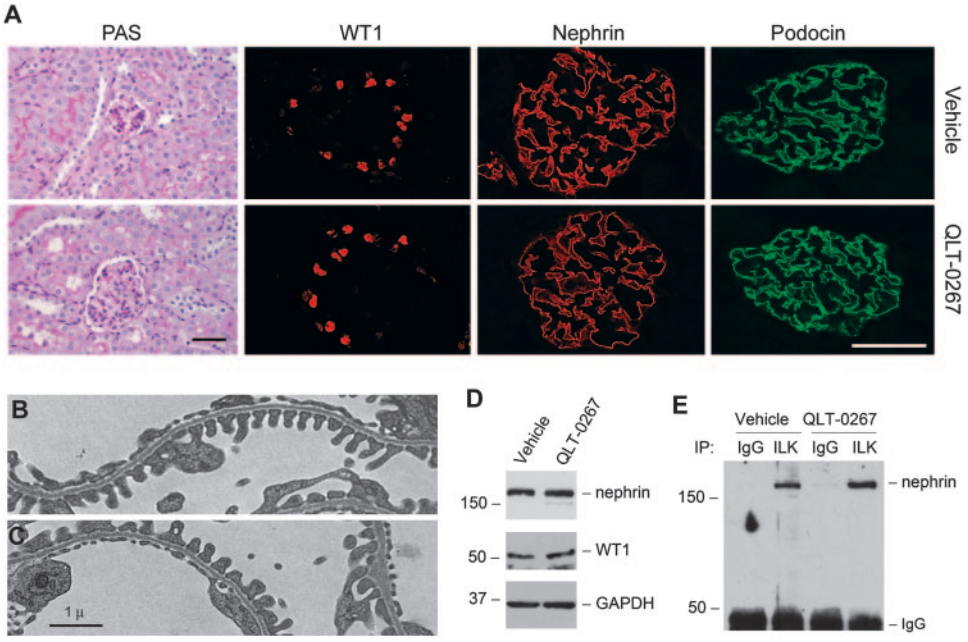

Figure 5. Inhibition of ILK activity does not affect normal kidney structure and nephrin/ILK interaction *in vivo*. (A) QLT-0267 does not affect kidney morphology, WT1-positive podocytes numbers, and nephrin and podocin expression and distribution *in vivo*. Mice were injected with QLT-0267 at 10 mg/kg body wt for 14 d, and kidney sections were subjected to routine periodic acid-Schiff (PAS) staining, as well as immunofluorescence staining for WT1, nephrin, and podocin, respectively. Bar = 30 μm. (B and C) Electron microscopy exhibits an intact ultrastructure of podocyte foot processes and glomerular basement membrane in vehicle (B) or QLT-0267–treated mice (C). Bar = 1 μm. (D) Western blot analysis shows the abundance of nephrin and WT1 in the glomeruli of mice injected with vehicle or QLT-0267. Glomerular lysates (pooled from five mice per group) were immunoblotted with antibodies against nephrin, WT1, and glyceraldehyde-3-phosphate dehydrogenase (GAPDH), respectively. (E) Co-immunoprecipitation demonstrates that administration of QLT-0267 *in vivo* did not affect ILK interaction with nephrin. Glomerular lysates (pooled from five mice per group) were immunoprecipitated with anti-ILK or control IgG, followed by immunoblotting with anti-nephrin.

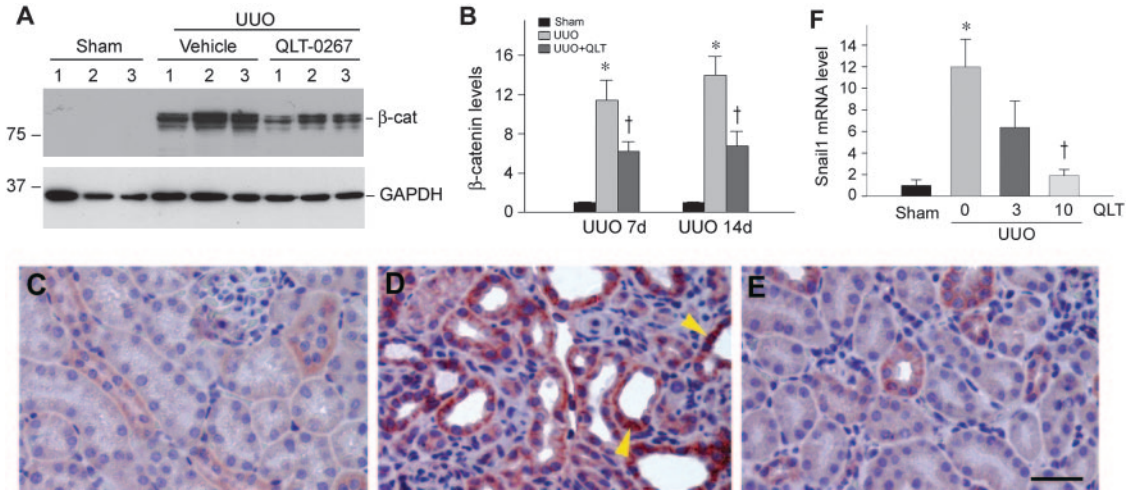

Figure 6. Inhibition of ILK by QLT-0267 reduces β-catenin accumulation and inhibits Snail1 expression in obstructive nephropathy. (A) Representative Western blot demonstrates that QLT-0267 administration significantly reduced β-catenin abundance in the obstructed kidney at 7 d after UUO. Numbers denote each individual mouse in a given group. (B) Graphic presentation shows the relative abundance of β-catenin in various groups as indicated. Data are means ± SEM of five animals per group. *$P < 0.05$ *versus* sham controls; †$P < 0.05$ *versus* vehicle controls. (C through E) Immunohistochemical staining shows β-catenin localization in different groups. (C) Sham controls. (D) UUO 7d. (E) UUO 7d injected with QLT-0267. Bar = 40 μm. Arrowheads indicate nuclear staining of β-catenin. (F) Quantitative determination of renal Snail1 mRNA levels by real-time RT-PCR in various groups as indicated. Relative renal Snail1 mRNA levels (fold induction *versus* sham controls) were presented. *$P < 0.05$ *versus* sham controls; †$P < 0.05$ *versus* vehicle controls. The dosages of QLT-0267 (mg/kg body wt) are given.

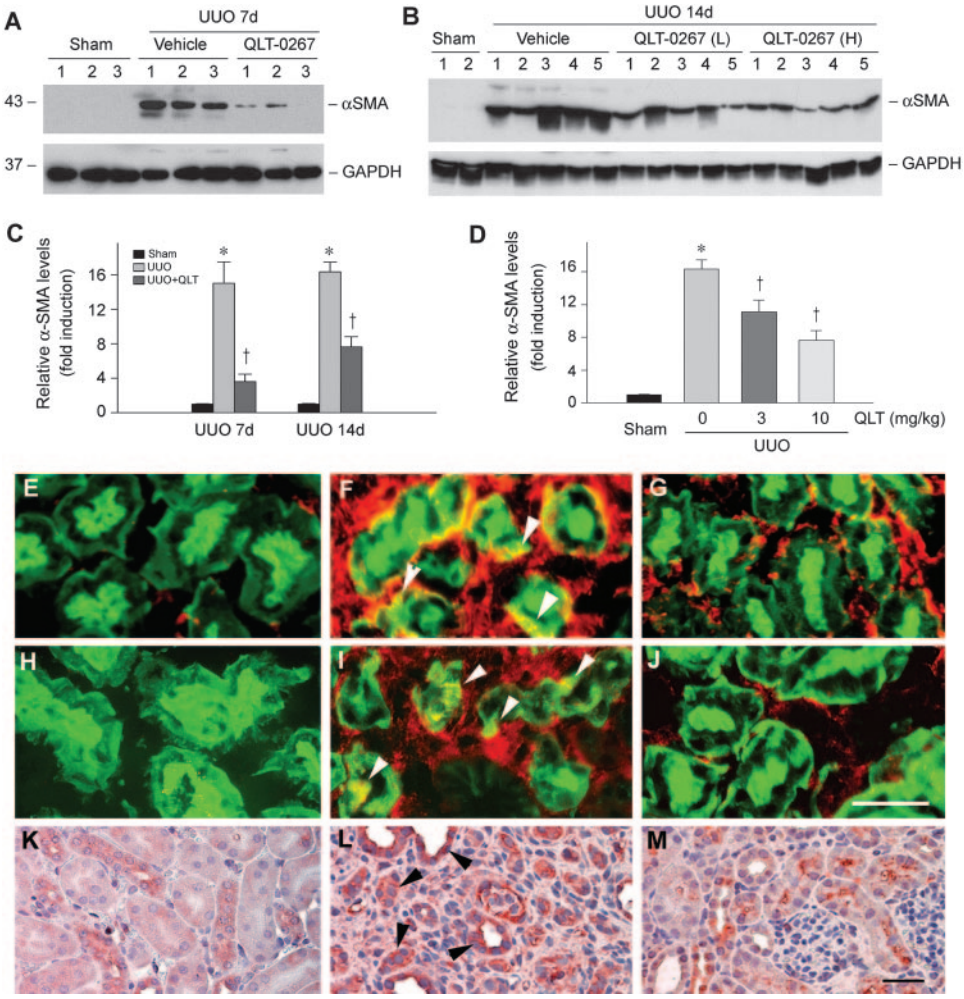

Figure 7. Inhibition of ILK by QLT-0267 blocks myofibroblast activation and tubular expression of α-SMA, fibronectin, and vimentin in mouse model of obstructive nephropathy. (A and B) Western blot demonstrates that QLT-0267 administration significantly inhibited α-SMA expression in the obstructed kidney after UUO. Kidney tissue lysates were immunoblotted with specific antibodies against α-SMA and GAPDH, respectively. Numbers denote each individual mouse in a given group. QLT-0267 (L), 3 mg/kg body wt. QLT-0267 (H), 10 mg/kg body wt. (C and D) Graphic presentation shows that QLT-0267 inhibited renal α-SMA expression in a time-dependent (C) and dosage-dependent manner (D). Data are means ± SEM of five animals per group. *$P < 0.05$ *versus* sham controls; †$P < 0.05$ *versus* vehicle controls. (E through J) Immunofluorescence staining shows α-SMA (red; E through G) or fibronectin (red; H through J) and tubular cell marker lectin (green) localization in different groups. (E and H) Sham controls. (F and I) UUO 7d with vehicle. (G and J) UUO 7d with QLT-0267. Arrowheads denote tubular expression of α-SMA or fibronectin, respectively. Bar = 30 μm. (K through M) Immunohistochemical staining shows vimentin expression in different groups. (K) Sham controls. (L) UUO 7d with vehicle. (M) UUO 7d with QLT-0267. Arrowheads denote tubular expression of vimentin. Bar = 30 μm.

hallmark of myofibroblasts.[28] Interestingly, administration of QLT-0267 largely blocked renal α-SMA expression (Figure 7, A and B). The inhibitory effects of QLT-0267 on α-SMA expression were both time (Figure 7C) and dosage dependent (Figure 7D). Similar results were obtained when using an indirect immunofluorescence staining for α-SMA (Figure 7, E through G). Notably, inhibition of ILK activity by QLT-0267 prevented tubular expression of α-SMA *in vivo* (Figure 7F, arrowheads).

We also examined the expression of fibronectin and vimentin in the obstructed kidney. Renal expression of fibronectin and vimentin was markedly induced after UUO, compared with sham controls (Figure 7, H through M). Co-localization studies revealed a clear tubular expression of fibronectin after obstructive injury (Figure 7I, arrowheads), in addition to its expression in the interstitium. Interestingly, the expression of vimentin, a mesenchymal marker, was primarily induced in renal tubules (Figure 7L, arrowheads). Administration of QLT-0267, however, inhibited the tubular expression of both fibronectin and vimentin in the obstructed kidneys (Figure 7, J and M).

Inhibition of ILK Activity Represses Matrix Gene Expression and Reduces Interstitial Fibrosis In Vivo

We assessed the effects of QLT-0267 on matrix production and

renal fibrosis in obstructive nephropathy. As shown in Figure 8, A and B, a dramatic induction of type I and type III collagen mRNA was observed in the obstructed kidney after UUO, when compared with sham controls. Administration of QLT-0267 significantly inhibited type I and type III collagen expression, as demonstrated by the quantitative, real-time reverse transcriptase–PCR (RT-PCR) approach (Figure 8B). Consistently, UUO caused a marked increase in collagen accumulation and deposition, as shown by a collagen-specific Picrosirius red staining (Figure 8, C and D). Treatment with QLT-0267, however, reduced the collagen deposition (Figure 8E). Quantitative determination of tissue total collagen content also confirmed a reduced collagen accumulation after QLT-0267 treatment (Figure 8F). Together, these results indicate that administration of ILK inhibitor QLT-0267 suppresses interstitial matrix overproduction and reduces renal fibrosis in experimental nephropathy *in vivo*.

DISCUSSION

The results presented in this study demonstrate that a hyperactive ILK plays an important role in mediating tubular EMT and the pathogenesis of renal fibrosis. We show that TGF-β1 induces a biphasic ILK activation in renal tubular epithelial cells, and blockade of ILK activity with a small-molecule inhibitor blunts ILK signaling and prevents tubular EMT *in vitro*. Furthermore, administration of ILK inhibitor *in vivo* significantly attenuates matrix production and reduces renal fibrosis in obstructive nephropathy, an aggressive model of renal interstitial fibrosis characterized by tubular EMT, myofibroblast activation, and excessive matrix deposition.[19,29] Our findings shed new light on the mechanism governing tubular EMT and the evolution of chronic kidney fibrosis and illustrate that targeting hyperactive ILK activity could be exploited as a new class of therapeutic modality for the treatment of fibrotic kidney diseases.

ILK is widely known for its dual biologic functions: As a scaffolding/adaptor protein that assembles a ternary protein complex through interacting with different protein partners and as a serine/threonine protein kinase that phosphorylates several intracellular signal mediators.[1,4] The contribution and relative importance of each of these two functions to a given cellular process is a matter of debate and likely context dependent.[1,2] Although the role of ILK as a key intracellular mediator that controls tubular EMT is well established,[9] the contribution of its kinase activity to this process remains to be fully elucidated. In this regard, this study represents the first examination of ILK kinase activity during the course of tubular EMT induced by TGF-β1. It is of interest to note that the kinetics of ILK activation after TGF-β1 stimulation reveals a biphasic pattern (Figure 1). Whereas the second wave of ILK activation is closely correlated with and likely contributed by its protein induction after TGF-β1 incubation, the early activation of ILK kinase is clearly independent of its protein abundance. These data suggest that the early activation of ILK is primarily triggered by an intracellular signaling event in an immediately early manner. At this stage, the exact upstream kinase respon-

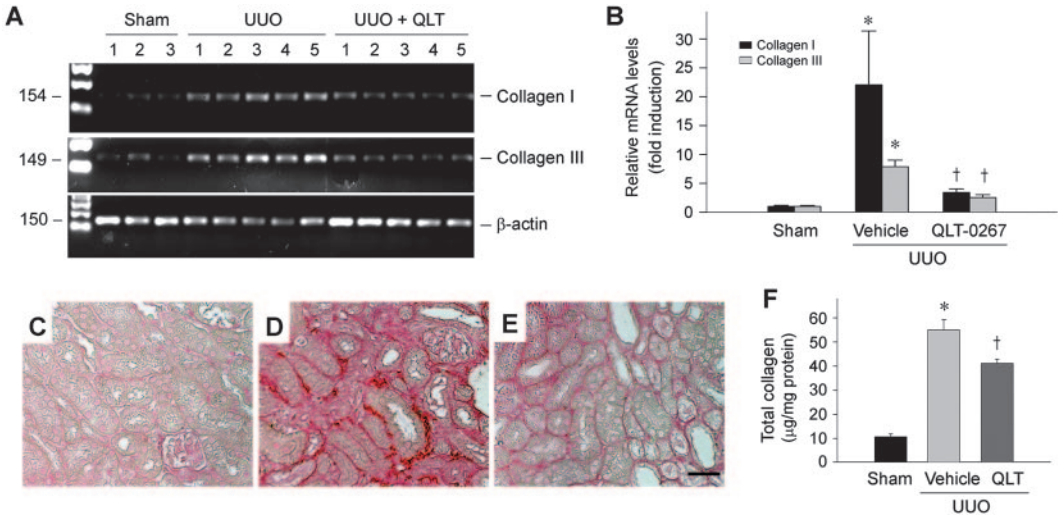

Figure 8. Inhibition of ILK by QLT-0267 suppresses type I and type III collagen expression and ameliorates interstitial collagen deposition and renal fibrosis after UUO. (A) Representative RT-PCR analysis of renal mRNA levels of type I and type III collagen in different groups as indicated. Numbers denote each individual mouse in a given group. (B) Quantitative determination of renal mRNA levels of interstitial collagens by real-time RT-PCR in various groups as indicated. Relative mRNA levels (fold induction *versus* sham controls) were presented. *$P < 0.05$ *versus* sham controls; †$P < 0.05$ *versus* vehicle controls. (C through E) Representative micrographs show the deposition of collagen as detected by Picrosirius red staining. (C) Sham controls. (D) UUO 7d. (E) UUO 7d injected with QLT-0267. Bar = 40 μm. (F) Inhibition of ILK by QLT-0267 reduced tissue total collagen deposition in the obstructed kidney at 7 d after UUO. Total collagen was measured and expressed as the ratio of collagen per total protein (μg/mg). *$P < 0.05$ *versus* sham controls; †$P < 0.05$ *versus* vehicle.

sible for the early ILK activation in HKC-8 cells remains to be characterized; however, TGF-β1–activated phosphatidylinositol 3-kinase (PI3K) seems to be the putative candidate, because earlier studies demonstrate that inhibitors of PI3K reduces ILK activity in cell lysate immunoprecipitates and ectopic expression of the PI3K catalytic subunit increases ILK-dependent kinase activity.[8] Regardless of the mechanism involved, these findings uncover that TGF-β1 not only induces ILK protein expression as previously reported[9] but also activates ILK kinase activity in a biphasic pattern.

The importance of ILK activation in tubular EMT is unambiguously illustrated by the observation that a highly selective small-molecule ILK inhibitor hampers tubular epithelial cell phenotypic conversion after TGF-β1 stimulation, despite that it does not affect Smad signaling (Figure 2E). This is consistent with a previous study in which the kinase-dead mutant of ILK reduced TGF-β1–induced tubular EMT in a dominant negative manner[9]; therefore, it is becoming apparent that ILK kinase activity is obligatory for mediating tubular EMT induced by TGF-β1. Thus far, numerous ILK kinase substrates have been identified.[1,30,31] Of them, Akt and GSK-3β are two most widely studied and recognized downstream effector kinases. ILK is shown to bind directly to and phosphorylate Akt on Ser473.[7] Likewise, ILK can directly phosphorylate GSK-3 on Ser9, causing its inhibition, which leads to the stabilization of β-catenin and stimulation of the activity of activator protein 1 (AP-1) and cAMP response element binding protein.[8,31,32] Stabilization of β-catenin results in its nuclear accumulation, wherein it associates with T cell factor/lymphoid enhancer–binding factor to regulate the EMT-related genes,[12,31,33] whereas AP-1 activation by ILK leads to stimulation of MMP expression.[34] Because GSK-3β is a downstream substrate for Akt, ILK also induces GSK-3β phosphorylation indirectly *via* Akt route. In this context, inhibition of ILK activity by QLT-0267 has targeted, directly or indirectly, several key molecular events in the processes of tubular EMT. This notion is supported by the observation that QLT-0267 inhibits TGF-β1–induced fibronectin, Snail1, and MMP-2 expression and restores E-cadherin and ZO-1 expression in HKC-8 cells. Notably, blockade of ILK signaling is unable to restore completely E-cadherin and ZO-1 expression in tubular epithelial cells in the presence of TGF-β1 (Figure 3). This is likely because the inhibitor of differentiation 1, a dominant negative antagonist of the basic helix-loop-helix transcription factors, is responsive to TGF-β1 stimulation and inhibits E-cadherin and ZO-1 expression as well by a mechanism independent of ILK signaling.[35]

Recent studies indicate an important role for ILK in podocyte biology, because conditional knockout of ILK in podocytes in mice results in massive proteinuria, glomerulosclerosis, and premature death.[26,27] We further uncovered that ILK, as a scaffolding protein, interacts with nephrin to form a ternary protein complex that connects the integrin and slit diaphragm signaling, and thus ablation of ILK leads to nephrin mislocalization and podocyte dysfunction.[27] It seems that the action of ILK as a scaffolding protein is independent of its kinase activity, because inhibition of ILK activity by QLT-0267 does not affect either ILK/nephrin interaction *in vivo* or nephrin distribution and glomerular filtration integrity (Figure 5, Table 1). These results strongly support our previous finding that the scaffolding function of ILK is essential for establishing the integrin/slit diaphragm connection in podocytes under physiologic conditions. Of note, ILK-mediated protein interaction usually does not necessitate its kinase activity, as demonstrated in several studies using different experimental systems.[1,36] In fact, ILK fragment lacking its kinase domain is still sufficient for interacting with its partners[36,37]; therefore, despite a vital role for ILK as a scaffolding protein in podocyte biology, inhibition of ILK activity by QLT-0267 *in vivo* seems quite safe and not to cause any adverse effects in mice (Table 1, Figure 5).

This study provides the first *in vivo* evidence that targeting ILK activity is beneficial and able to retard the progression of chronic kidney diseases. Given its ability to block EMT, it is not surprising that administration of ILK inhibitor QLT-0267 prevents myofibroblast activation, suppresses the expression of interstitial matrix components such as type I and type III collagen and fibronectin, and reduces total tissue collagen content in obstructive nephropathy induced by UUO. On the basis of *in vitro* data, it is conceivable that the beneficial effect of ILK inhibitor QLT-0267 is mediated primarily by its ability to block EMT. This speculation is further strengthened by numerous observations. First, a previous report indicated that ILK is predominantly expressed and specifically induced in renal tubular epithelium after obstructive injury in a mouse model of UUO.[9] Second, tubular EMT is an imperative pathogenic mechanism by which more than one third of the matrix-producing cells are derived from proximal tubules in this model, as previously reported.[29] Third, reduction of renal fibrosis after QLT-0267 administration is associated with the suppression of β-catenin and Snail1, key EMT-regulatory genes (Figure 6).[22,23,38] Indeed, tubular expression of mesenchymal markers such as α-SMA, vimentin, and fibronectin after UUO is suppressed by QLT-0267 *in vivo* (Figure 7, E through M). Nonetheless, we cannot exclude the possibility that ILK inhibitor may protect kidney tissue from fibrotic lesions by other mechanisms as well. In that regard, one study demonstrated that tissue-type plasminogen activator promotes renal myofibroblast activation through the LDL receptor–related protein 1–mediated recruitment of β1 integrin/ILK signaling[39]; therefore, it is plausible that ILK inhibitor may attenuate renal interstitial fibrosis, at least in part, by suppressing myofibroblast activation from quiescent fibroblasts *in vivo*.

Renal interstitial fibrosis is considered a common outcome of a wide variety of chronic kidney diseases with diverse causes, and it is presently incurable.[40,41] This study, together with previous reports,[6,9] illustrates that by deciphering the key pathway and its mediators in renal fibrogenesis, it is plausible to develop a completely new class of therapeutic modality for hampering the fibrotic destruction of kidney structure and function after

injury. Because hyperactive ILK is implicated in the pathogenesis of various nephropathies, targeting ILK signaling with small-molecule inhibitor might be therapeutically effective in other models of chronic kidney diseases as well. Clearly, more studies are needed in the future in this area.

CONCISE METHODS

Cell Culture and Treatment

HKC-8 were cultured in DMEM-Ham's F12 medium supplemented with 5% FBS, as described previously.[20] HKC-8 cells were serum-starved for 16 h and then treated without or with recombinant TGF-β1 (R&D Systems, Minneapolis, MN) and/or a high-selective, small-molecule ILK inhibitor QLT-0267 (QLT, Vancouver, BC, Canada) for various periods of time as indicated. The specificity and selectivity of QLT-0267 were reported previously.[18] The cells were then collected for *in vitro* kinase assay, Western blot analysis, and immunofluorescence staining. All other chemicals were of analytic grade and were obtained from Sigma (St. Louis, MO) or Fisher (Pittsburgh, PA) unless otherwise indicated.

Animal Model

Male CD-1 mice weighing approximately 20 to 22 g were obtained from Harlan Sprague-Dawley (Indianapolis, IN). To study the potential effect of ILK inhibition on normal kidney structure and function, we subjected mice to daily intraperitoneal injection of vehicle or QLT0267 at 10 mg/kg body wt for 14 d. Body weight and kidney weight were recorded at the time of killing. Urine albumin and total protein levels were determined. UUO was performed using an established protocol, as described previously.[42] QLT-0267 was administered by daily intraperitoneal injection at the dosages of 3 and 10 mg/kg body wt, respectively. Groups of mice ($n = 5$) were killed at 7 and 14 d after UUO, and the kidney tissues were removed for various analyses. All animal protocols were approved by the institutional animal care and use committee at the University of Pittsburgh.

Western Blot Analysis

Western blot analysis for specific protein expression was performed essentially according to an established procedure.[19] The primary antibodies used were as follows: Anti-ILK (05-592; Millipore, Billerica, MA); antibodies against phospho-Akt (Ser473), total Akt, phospho-GSK-3β (Ser9), total GSK-3β, and phospho-Smad3 (cat. no. 9514; Cell Signaling Technology., Beverly, MA); anti–PAI-1 (sc-5297), anti-WT1 (sc-192), and anti-actin (sc-1616; Santa Cruz Biotechnology, Santa Cruz, CA); anti–cyclin D1 (DCS-6; Lab Vision Corp., Fremont, CA); anti–α-SMA (clone 1A4) and anti–α-tubulin (Sigma, St. Louis, MO); anti–E-cadherin (clone 36), anti-fibronectin (clone 10), anti–β-catenin (cat. no. 610154), and anti–PINCH-1 (cat no. 612711; BD Transduction Laboratories, San Jose, CA); anti-nephrin (GP-N2; Progen, Heidelberg, Germany); and anti–glyceraldehyde-3-phosphate dehydrogenase (Ambion, Austin, TX). Quantification was performed by measurement of the intensity of the signals with the use of National Institutes of Health Image analysis software.

In Vitro ILK Kinase Assay

HKC-8 cells were treated with recombinant TGF-β1 for various periods of time at the concentration of 2 ng/ml. Cells were lysed in NP-40 lysis buffer for 30 min. Cell lysates (250 μg) were precleared and then immunoprecipitated with 5 μg of polyclonal anti-ILK antibody. The immunocomplexes were washed twice with kinase assay buffer containing 50 mM HEPES (pH 7.5), 10 mM $MgCl_2$, and 2 mM $MnCl_2$. The kinase assay was performed by incubating at 30°C for 25 min in 25 μl of reaction buffer containing 5 μCi γ-^{32}P-ATP and 5 μg of myelin basic protein (Millipore).[3] Reactions were stopped by boiling in 10 μl of 4× SDS sample buffer. Samples were separated on a 15% SDS-polyacrylamide gel and visualized by autoradiography.

Immunofluorescence and Immunohistochemical Staining

Indirect immunofluorescence staining was performed using an established procedure.[19] Briefly, cells cultured on coverslips were fixed with cold methanol:acetone (1:1) for 10 min at −20°C and blocked with 20% normal donkey serum in PBS buffer for 30 min. Cells were then incubated with the specific primary antibodies against fibronectin and anti–ZO-1 (61-7300; Invitrogen, Carlsbad, CA). Kidney cryosections were prepared at 5-μm thickness and fixed for 10 min with cold methanol:acetone (1:1). Sections were incubated with anti–α-SMA (ab5694; Abcam, Cambridge, MA); anti-fibronectin (sc-9068), anti-WT1 (sc-192), and anti-podocin (sc-22298; Santa Cruz Biotechnology); and anti-nephrin (GP-N2; Progen). To visualize the primary antibodies, we stained cells and cryosections with cyanine Cy2- or Cy3-conjugated secondary antibodies (Jackson ImmunoResearch Laboratories, West Grove, PA). Immunohistochemical staining of kidney sections was performed by using anti–β-catenin (ab-15180; Abcam) and anti-vimentin (V-6630; Sigma) antibodies with the Vector M.O.M. immunodetection kit, according to the protocol specified by the manufacturer (Vector Laboratories, Burlingame, CA). As a negative control, the primary antibody was replaced with nonimmune IgG, and no staining occurred. For some samples, cells were double stained with DAPI (4′, 6-diamidino-2-phenylindole, HCl) to visualize the nuclei. Kidney cryosections were also stained with renal proximal tubular marker fluorescein-conjugated lectin from *Tephrosia purpurea* (Sigma). Stained cells and cryosections were mounted with Vectashield mounting medium (Vector Laboratories) and viewed with a Nikon Eclipse E600 microscope equipped with a digital camera (Melville, NY).

RT-PCR and Real-Time RT-PCR

Total RNA was extracted using TRIzol RNA isolation system (Invitrogen). The first strand of cDNA was synthesized using 2 μg of RNA in 20 μl of reaction buffer by reverse transcription using AMV-RT (Promega, Madison, WI) and random primers at 42°C for 30 min. PCR was carried out using a standard PCR kit and 1-μl aliquot of cDNA, HotStarTaq polymerase (Qiagen, Valencia, CA) with specific primer pairs. The sequences of the primer pairs for mouse collagen I and collagen III and mouse and human β-actin were described previously.[22] The sequences of other primer pairs were as follows: PAI-1, 5′-GGC CAT TAC TAC GAC ATC CTG-3′ (sense) and 5′-GGT CAT GTT GCC TTT CCA GT-3′ (antisense); MMP-2, 5′-CTT CCA GGG CAC ATC CTA

TG-3′ (sense) and 5′-CCT TCT GAG TTC CCA CCA AC-3′ (antisense). For quantitative determination of mRNA levels, a real-time RT-PCR was performed on ABI PRISM 7000 Sequence Detection System (Applied Biosystems, Foster City, CA), as described previously.[43] The PCR reaction mixture in a 25-μl volume contained 12.5 μl of 2× SYBR Green PCR Master Mix (Applied Biosystems), 5 μl of diluted RT product (1:10), and 0.5 μM sense and antisense primer sets. The primer pairs for mouse collagen I and III were the same as those used in regular RT-PCR. The sequences of β-actin primer pairs used in real-time PCR were described previously.[43] The sequences of Snail1 primer pairs were as follows: Human Snail1, 5′-AGG ATC TCC AGG CTC GAA AG (sense) and 5′-GTA GCA GCC AGG GCC TAG AG (antisense); mouse Snail1, 5′-ATT CTC CTG CTC CCA CTG C (sense) and 5′-GAC TCT TGG TGC TTG TGG AG (antisense). PCR reaction was run by using standard conditions. After sequential incubations at 50°C for 2 min and 95°C for 10 min, respectively, the amplification protocol consisted of 50 cycles of denaturing at 95°C for 15 s, and annealing and extension at 60°C for 60 s. The standard curve was made from series dilutions of template cDNA. The mRNA levels of various genes were calculated after normalizing with β-actin.

Gelatin Zymographic Analysis

Zymographic analysis of MMP proteolytic activity in the supernatant of cultured cells was performed according to the method described previously.[20] HKC-8 cells were treated with TGF-β1 (1 ng/ml) and/or QLT-0267 (5 μM), and conditioned media were collected after 48 h of incubation. A constant amount of protein from the conditioned media (15 μg) was loaded into 10% SDS-polyacrylamide gel containing 1 mg/ml gelatin (Bio-Rad, Hercules, CA). After electrophoresis, SDS was removed from the gel by incubation in 2.5% Triton X-100 for 30 min with gentle shaking. The gel was incubated at 37°C for 16 to 36 h in a developing buffer containing 50 mM Tris-HCl (pH 7.6), 0.2 M NaCl, 5 mM $CaCl_2$, and 0.02% Brij 35. The gel was then stained with a solution of 30% methanol, 10% glacial acetic acid, and 0.5% Coomassie blue G250, followed by destaining in the same solution without dye. Proteinase activity was detected as unstained bands on a blue background representing areas of gelatin digestion.

Urine Albumin, Total Protein, and Creatinine Assay

Urine total protein levels were determined using a bicinconinic acid–based protein assay kit (Sigma) with BSA as a standard. Urine albumin was measured by using a mouse Albumin ELISA Quantitation kit, according to the manufacturer's protocol (Bethyl Laboratories, Montgomery, TX). Serum and urine creatinine was determined by a routine procedure as described previously.[27]

Electron Microscopy

Electron microscopy of kidney samples was carried out by routine procedures as described previously.[27] Ultrathin sections were observed and photographed using a JEOL JEM 1210 transmission electron microscope (JEOL, Peabody, MA).

Co-immunoprecipitation

Glomeruli were isolated by conventional differential sieving technique from the mice receiving daily injection of vehicle or QLT0267 at 10 mg/kg body wt for 14 d. Nephrin/ILK interaction was assessed by co-immunoprecipitation using an established method.[27] Briefly, isolated glomeruli were lysed on ice in 1 ml of nondenaturing lysis buffer containing 1% Triton X-100, 0.01 M Tris-HCl (pH 8.0), 0.14 M NaCl, 0.025% NaN_3, 1% protease inhibitor cocktail, and 1% phosphatase inhibitors cocktail I and II (Sigma). Glomerular lysates were incubated overnight at 4°C with 4 μg of anti-ILK (Upstate, Lake Placid, NY), followed by precipitation with 30 μl of protein A/G Plus-Agarose for 1 h at 4°C. The precipitated complexes were immunoblotted with anti-nephrin antibody (GP-N2; Progen).

Quantitative Determination of Collagen and Total Protein

For quantitative measurement of collagen and total protein, 4-μm sections of paraffin-embedded tissue were stained with Sirius red F3BA and Fast green FCF (Sigma) for collagen and noncollagen protein content. After eluting the dye from tissue sections with sodium hydroxide-methanol, the absorbances of 540 and 605 nm were determined for Sirius red F3BA and Fast green FCF binding protein, respectively. This assay provided a simple, relative measurement of the ratio of collagen/total protein.[22] The relative amount of collagen in the samples was calculated and expressed as micrograms per milligram of total protein.

Statistical Analyses

All data examined were expressed as means ± SEM. Statistical analyses of the data was performed using SigmaStat software (Jandel Scientific Software, San Rafael, CA). Comparison between groups was made using one-way ANOVA, followed by Student-Newman-Keuls test. $P < 0.05$ was considered significant.

ACKNOWLEDGMENTS

This work was supported by National Institutes of Health grants DK061408, DK064005, and DK071040. X.T. was supported by a postdoctoral fellowship from American Heart Association Greater Rivers Affiliate.

DISCLOSURES

None.

REFERENCES

1. Legate KR, Montanez E, Kudlacek O, Fassler R: ILK, PINCH and parvin: The tIPP of integrin signaling. *Nat Rev Mol Cell Biol* 7: 20–31, 2006
2. Hannigan G, Troussard AA, Dedhar S: Integrin-linked kinase: A cancer therapeutic target unique among its ILK. *Nat Rev Cancer* 5: 51–63, 2005
3. Hannigan GE, Leung-Hagesteijn C, Fitz-Gibbon L, Coppolino MG, Radeva G, Filmus J, Bell JC, Dedhar S: Regulation of cell adhesion and anchorage-dependent growth by a new beta 1-integrin-linked protein kinase. *Nature* 379: 91–96, 1996
4. Wu C: The PINCH-ILK-parvin complexes: Assembly, functions and regulation. *Biochim Biophys Acta* 1692: 55–62, 2004
5. Tu Y, Li F, Goicoechea S, Wu C: The LIM-only protein PINCH directly

interacts with integrin-linked kinase and is recruited to integrin-rich sites in spreading cells. *Mol Cell Biol* 19: 2425–2434, 1999
6. Li Y, Dai C, Wu C, Liu Y: PINCH-1 promotes tubular epithelial-to-mesenchymal transition by interacting with integrin-linked kinase. *J Am Soc Nephrol* 18: 2534–2543, 2007
7. Persad S, Attwell S, Gray V, Mawji N, Deng JT, Leung D, Yan J, Sanghera J, Walsh MP, Dedhar S: Regulation of protein kinase B/Akt-serine 473 phosphorylation by integrin-linked kinase: Critical roles for kinase activity and amino acids arginine 211 and serine 343. *J Biol Chem* 276: 27462–27469, 2001
8. Delcommenne M, Tan C, Gray V, Rue L, Woodgett J, Dedhar S: Phosphoinositide-3-OH kinase-dependent regulation of glycogen synthase kinase 3 and protein kinase B/AKT by the integrin-linked kinase. *Proc Natl Acad Sci U S A* 95: 11211–11216, 1998
9. Li Y, Yang J, Dai C, Wu C, Liu Y: Role for integrin-linked kinase in mediating tubular epithelial to mesenchymal transition and renal interstitial fibrogenesis. *J Clin Invest* 112: 503–516, 2003
10. Guo L, Sanders PW, Woods A, Wu C: The distribution and regulation of integrin-linked kinase in normal and diabetic kidneys. *Am J Pathol* 159: 1735–1742, 2001
11. Kretzler M, Teixeira VP, Unschuld PG, Cohen CD, Wanke R, Edenhofer I, Mundel P, Schlondorff D, Holthofer H: Integrin-linked kinase as a candidate downstream effector in proteinuria. *FASEB J* 15: 1843–1845, 2001
12. Teixeira Vde P, Blattner SM, Li M, Anders HJ, Cohen CD, Edenhofer I, Calvaresi N, Merkle M, Rastaldi MP, Kretzler M: Functional consequences of integrin-linked kinase activation in podocyte damage. *Kidney Int* 67: 514–523, 2005
13. Liu BC, Li MX, Zhang JD, Liu XC, Zhang XL, Phillips AO: Inhibition of integrin-linked kinase *via* a siRNA expression plasmid attenuates connective tissue growth factor-induced human proximal tubular epithelial cells to mesenchymal transition. *Am J Nephrol* 28: 143–151, 2008
14. Li Y, Kang YS, Dai C, Kiss LP, Wen X, Liu Y: Epithelial-to-mesenchymal transition is a potential pathway leading to podocyte dysfunction and proteinuria. *Am J Pathol* 172: 299–308, 2008
15. Oloumi A, Syam S, Dedhar S: Modulation of Wnt3a-mediated nuclear beta-catenin accumulation and activation by integrin-linked kinase in mammalian cells. *Oncogene* 25: 7747–7757, 2006
16. Liu Y: Epithelial to mesenchymal transition in renal fibrogenesis: Pathologic significance, molecular mechanism, and therapeutic intervention. *J Am Soc Nephrol* 15: 1–12, 2004
17. Kalluri R, Neilson EG: Epithelial-mesenchymal transition and its implications for fibrosis. *J Clin Invest* 112: 1776–1784, 2003
18. Koul D, Shen R, Bergh S, Lu Y, de Groot JF, Liu TJ, Mills GB, Yung WK: Targeting integrin-linked kinase inhibits Akt signaling pathways and decreases tumor progression of human glioblastoma. *Mol Cancer Ther* 4: 1681–1688, 2005
19. Yang J, Liu Y: Blockage of tubular epithelial to myofibroblast transition by hepatocyte growth factor prevents renal interstitial fibrosis. *J Am Soc Nephrol* 13: 96–107, 2002
20. Yang J, Liu Y: Dissection of key events in tubular epithelial to myofibroblast transition and its implications in renal interstitial fibrosis. *Am J Pathol* 159: 1465–1475, 2001
21. Wu C, Keightley SY, Leung-Hagesteijn C, Radeva G, Coppolino M, Goicoechea S, McDonald JA, Dedhar S: Integrin-linked protein kinase regulates fibronectin matrix assembly, E-cadherin expression, and tumorigenicity. *J Biol Chem* 273: 528–536, 1998
22. Tan X, Li Y, Liu Y: Paricalcitol attenuates renal interstitial fibrosis in obstructive nephropathy. *J Am Soc Nephrol* 17: 3382–3393, 2006
23. Boutet A, De Frutos CA, Maxwell PH, Mayol MJ, Romero J, Nieto MA: Snail activation disrupts tissue homeostasis and induces fibrosis in the adult kidney. *EMBO J* 25: 5603–5613, 2006
24. Eddy AA, Fogo AB: Plasminogen activator inhibitor-1 in chronic kidney disease: Evidence and mechanisms of action. *J Am Soc Nephrol* 17: 2999–3012, 2006
25. Cheng S, Lovett DH: Gelatinase A (MMP-2) is necessary and sufficient for renal tubular cell epithelial-mesenchymal transformation. *Am J Pathol* 162: 1937–1949, 2003
26. El-Aouni C, Herbach N, Blattner SM, Henger A, Rastaldi MP, Jarad G, Miner JH, Moeller MJ, St-Arnaud R, Dedhar S, Holzman LB, Wanke R, Kretzler M: Podocyte-specific deletion of integrin-linked kinase results in severe glomerular basement membrane alterations and progressive glomerulosclerosis. *J Am Soc Nephrol* 17: 1334–1344, 2006
27. Dai C, Stolz DB, Bastacky SI, St-Arnaud R, Wu C, Dedhar S, Liu Y: Essential role of integrin-linked kinase in podocyte biology: Bridging the integrin and slit diaphragm signaling. *J Am Soc Nephrol* 17: 2164–2175, 2006
28. Strutz F, Zeisberg M: Renal fibroblasts and myofibroblasts in chronic kidney disease. *J Am Soc Nephrol* 17: 2992–2998, 2006
29. Iwano M, Plieth D, Danoff TM, Xue C, Okada H, Neilson EG: Evidence that fibroblasts derive from epithelium during tissue fibrosis. *J Clin Invest* 110: 341–350, 2002
30. Deng JT, Van Lierop JE, Sutherland C, Walsh MP: Ca2+-independent smooth muscle contraction: A novel function for integrin-linked kinase. *J Biol Chem* 276: 16365–16373, 2001
31. D'Amico M, Hulit J, Amanatullah DF, Zafonte BT, Albanese C, Bouzahzah B, Fu M, Augenlicht LH, Donehower LA, Takemaru K, Moon RT, Davis R, Lisanti MP, Shtutman M, Zhurinsky J, Ben-Ze'ev A, Troussard AA, Dedhar S, Pestell RG: The integrin-linked kinase regulates the cyclin D1 gene through glycogen synthase kinase 3beta and cAMP-responsive element-binding protein-dependent pathways. *J Biol Chem* 275: 32649–32657, 2000
32. Joshi MB, Ivanov D, Philippova M, Erne P, Resink TJ: Integrin-linked kinase is an essential mediator for T-cadherin-dependent signaling *via* Akt and GSK3beta in endothelial cells. *FASEB J* 21: 3083–3095, 2007
33. Kim K, Lu Z, Hay ED: Direct evidence for a role of beta-catenin/LEF-1 signaling pathway in induction of EMT. *Cell Biol Int* 26: 463–476, 2002
34. Troussard AA, Costello P, Yoganathan TN, Kumagai S, Roskelley CD, Dedhar S: The integrin linked kinase (ILK) induces an invasive phenotype *via* AP-1 transcription factor-dependent upregulation of matrix metalloproteinase 9 (MMP-9). *Oncogene* 19: 5444–5452, 2000
35. Li Y, Yang J, Luo JH, Dedhar S, Liu Y: Tubular epithelial cell dedifferentiation is driven by the helix-loop-helix transcriptional inhibitor Id1. *J Am Soc Nephrol* 18: 449–460, 2007
36. Guo L, Wu C: Regulation of fibronectin matrix deposition and cell proliferation by the PINCH-ILK-CH-ILKBP complex. *FASEB J* 16: 1298–1300, 2002
37. Wu C: PINCH, N (i) ck and the ILK: Network wiring at cell-matrix adhesions. *Trends Cell Biol* 15: 460–466, 2005
38. Yoshino J, Monkawa T, Tsuji M, Inukai M, Itoh H, Hayashi M: Snail1 is involved in the renal epithelial-mesenchymal transition. *Biochem Biophys Res Commun* 362: 63–68, 2007
39. Hu K, Wu C, Mars WM, Liu Y: Tissue-type plasminogen activator promotes murine myofibroblast activation through LDL receptor-related protein 1-mediated integrin signaling. *J Clin Invest* 117: 3821–3832, 2007
40. Liu Y: Renal fibrosis: New insights into the pathogenesis and therapeutics. *Kidney Int* 69: 213–217, 2006
41. Eddy AA: Molecular basis of renal fibrosis. *Pediatr Nephrol* 15: 290–301, 2000
42. Yang J, Dai C, Liu Y: Hepatocyte growth factor gene therapy and angiotensin II blockade synergistically attenuate renal interstitial fibrosis in mice. *J Am Soc Nephrol* 13: 2464–2477, 2002
43. Li Y, Wen X, Spataro BC, Hu K, Dai C, Liu Y: Hepatocyte growth factor is a downstream effector that mediates the antifibrotic action of peroxisome proliferator-activated receptor-γ agonists. *J Am Soc Nephrol* 17: 54–65, 2006